

Dislocations and the enhancement of superconductivity in odd-parity superconductor Sr_2RuO_4

Y. A. Ying,¹ N. E. Staley,¹ Y. Xin,² K. Sun,³ X. Cai,¹ D. Fobes,⁴ T. Liu,⁴ Z. Q. Mao,⁴ and Y. Liu^{1,*}

¹*Department of Physics and Materials Research Institute,*

The Pennsylvania State University, University Park, Pennsylvania 16802, USA

²*National High Magnetic Field Laboratory, Florida State University, Tallahassee, Florida 32306, USA*

³*Condensed Matter Theory Center and Joint Quantum Institute,*

Department of Physics, University of Maryland, College Park, Maryland 20742, USA

⁴*Department of Physics, Tulane University, New Orleans, Louisiana 70118, USA*

(Dated: March 4, 2013)

We report observation of the enhancement of superconductivity near lattice dislocations and the absence of the strengthening of vortex pinning in odd-parity superconductor Sr_2RuO_4 , both surprising results in direct contrast to the well known sensitivity of superconductivity in Sr_2RuO_4 to disorder. The enhanced superconductivity appears to be related fundamentally to the two-component nature of the superconducting order parameter, as revealed in our phenomenological theory taking into account the effect of symmetry reduction near a dislocation.

PACS numbers: 74.70.Pq, 61.72.Ff, 74.20.De, 74.25.Sv

Sr_2RuO_4 , a leading candidate for a textbook example of unconventional superconductors[1–5], has attracted much attention in recent years in condensed matter physics and beyond, including the pursuit of non-Abelian Majorana anyons[6, 7], key for topological quantum computing[8]. A large body of experimental data, including that obtained in phase sensitive measurements[9], has shown that the layered perovskite material Sr_2RuO_4 is a spin-triplet, odd-parity superconductor[4, 5]. Assuming that superconductivity in this material is two-dimensional (2D) in nature, the four-fold tetragonal crystalline symmetry dictates that the pairing symmetry in this superconductor must be one of the five representations[2]. Among those, only the two-component, $p_x \pm ip_y$ state is consistent with the muon spin rotation[10] and Kerr rotation[11] measurements that suggest the presence of a spontaneous magnetic field in the superconducting state of Sr_2RuO_4 , making it an electronic analog[2] of the superfluid ^3He A-phase and moreover a topological superconductor defined by the presence of gapless chiral edge states[6, 7]. An important question of interest is what is the microscopic mechanism responsible for such a highly exotic superconducting state. In this regard, models based on ferromagnetic[12] or antiferromagnetic fluctuations[13], spin-orbital coupling[14], interaction theory[15, 16], and Hund's rule coupling[3] have been proposed. The debate on these mechanisms is currently on going[5].

The eutectic phase of Sr_2RuO_4 -Ru featuring crystalline islands of Ru embedded in the bulk crystalline Sr_2RuO_4 , found previously to feature a T_c nearly double that of the bulk Sr_2RuO_4 [17], may provide insight into the mechanism issue. The T_c enhancement was attributed to the capillary effect at the interface between Ru and Sr_2RuO_4 [18]. It was more recently revealed that dislocations were abundant near a Ru island in bulk[19],

also seen here in Sr_2RuO_4 flakes [Fig. 1(a)] (See Supplemental Material for detailed sample preparation), leading to the intriguing question as to whether these dislocations also contribute to the enhancement of T_c [20]. An edge dislocation in a Sr_2RuO_4 lattice [Fig. 1(b)], near which the four-fold rotational symmetry is lost, is expected to lead to complicated modifications to the local lattice parameters and electronic states.

On the other hand, a phenomenological theory can be formulated to capture the effect of the symmetry reduction associated with a dislocation without spelling out explicitly the local microscopic properties. The free energy density of the bulk Sr_2RuO_4 with a four-fold tetragonal symmetry in zero magnetic field can be written as[18],

$$\begin{aligned}
 f = & a(|\eta_x|^2 + |\eta_y|^2) + b_1(|\eta_x|^2 + |\eta_y|^2)^2 \\
 & + \frac{b_2}{2}(\eta_x^{*2}\eta_y^2 + c.c.) + b_3|\eta_x|^2|\eta_y|^2 \\
 & + K_1(|\partial_x\eta_x|^2 + |\partial_y\eta_y|^2) + K_2(|\partial_x\eta_y|^2 + |\partial_y\eta_x|^2) \\
 & + [K_3(\partial_x\eta_x)^*(\partial_y\eta_y) + K_4(\partial_x\eta_y)^*(\partial_y\eta_x) + c.c.] \\
 & + K_5(|\partial_z\eta_x|^2 + |\partial_z\eta_y|^2)
 \end{aligned} \quad (1)$$

where η_x and η_y denote the two-component order parameter, $a(T) = \alpha(T - T_{c0})$, with α a constant and $T_{c0} = 1.5$ K the bulk T_c of Sr_2RuO_4 , b_i ($i = 1 - 3$) and K_j ($j = 1 - 5$) parameters characterizing the bulk superconductor. Consider now a bulk Sr_2RuO_4 crystal for which the four-fold rotational symmetry is lost because of, say, the application of an in-plane uniaxial strain. A set of parameters, m_1 and m_2 used to quantify the effect of lattice distortions and μ to measure the mixing of the two order parameter components, can be introduced to describe the symmetry breaking strength. To obtain only the superconducting transition temperature, it is sufficient to consider the free energy density up to

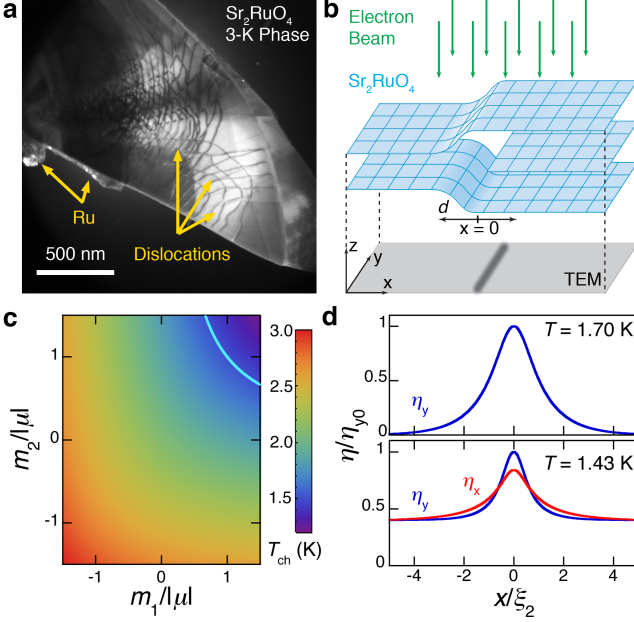


FIG. 1. (Color online) (a) Transmission electron microscopy (TEM) image of a Sr_2RuO_4 single-crystal flake showing Ru microdomains and dislocation lines. (b) Schematic of an edge dislocation caused by an extra layer in a Sr_2RuO_4 lattice. The edge dislocation scatters the electron beam in a TEM study, manifesting itself as a dark line in the TEM image. (c) T_{ch} plotted as a function of $m_1/|\mu|$ and $m_2/|\mu|$ for $|\mu|/\alpha = 0.4$. The value of T_{ch} is represented by a color scale. The highlighted curve represents the contour of $T_{ch} = 1.5$ K. (d) Spatial dependence of η_x and η_y normalized to the value of η_y at $x = 0$ for $T_1 = 1.7$ K, $T_2 = 1.43$ K, and $m_1/|\mu| = -1.5$, $m_2/|\mu| = -1.5$, $|\mu|/\alpha = 0.4$, respectively. Other parameters are $T_{c0} = 1.5$ K, $T_{ch} = 3$ K, $T_c = 1.9$ K, and $\xi_2(T_{1,2}) = [K_2/|\alpha|(T_{1,2} - T_{c0})]^{1/2}$, superconducting coherence lengths at finite temperatures.

the quadratic terms,

$$f_{RS} = (a + m_1)|\eta_x|^2 + (a + m_2)|\eta_y|^2 + \mu\eta_x^*\eta_y + \mu^*\eta_x\eta_y^* + \sum_{ijkl} \Gamma_{ijkl}\eta_i^*\eta_j^*\eta_k\eta_l \quad (2)$$

The modified transition temperature T_{ch} , determined by the eigenvalues of the quadratic terms, is given by

$$T_{ch} = T_{c0} + \frac{1}{\alpha} \left(\sqrt{m_-^2 + |\mu|^2} - m_+ \right) \quad (3)$$

where $m_{\pm} = (m_1 \pm m_2)/2$. Depending on the values of m_{\pm} , $T_{ch} > T_{c0}$ can be obtained [Fig. 1(c)].

Building on this result for a hypothetical bulk crystal of Sr_2RuO_4 with a broken four-fold symmetry, we proceed to analyze a more realistic model system featuring a single dislocation of a width d embedded in a bulk crystal, shown in Fig. 1(b). To begin with, we assume that the locally enhanced superconducting transition temperature within the dislocation is T_c , which is lower than

T_{ch} for the corresponding homogeneous bulk characterized by a set of the symmetry reduction parameters (m_1 , m_2 , and μ). To reach T_c , the effect of the bulk on the embedded dislocation region must be taken into account. This can be done by writing the free energy density for the dislocation region in the form of a δ -function

$$f_D = \delta(x)d\alpha(T - T_{c0})(|\eta_x|^2 + |\eta_y|^2) \quad (4)$$

employed successfully in the previous analysis of the capillary effect at the interface between Ru and Sr_2RuO_4 [18], and solving the linearized Ginzburg-Landau equations derived from Eq. (1). Matching the boundary conditions at $x = 0$ (see Supplemental Material), we found that T_c is given by the solution of

$$2\sqrt{\frac{K_2}{\alpha}(T_c - T_{c0})} = d(T_{ch} - T_c) \quad (5)$$

which requires that $T_c > T_{c0}$ and $T_{ch} > T_c$ for simple self consistency. Because the highest T_c found in Sr_2RuO_4 and the related eutectic systems is 3 K[5, 17], we assume that $T_{ch} = 3$ K. As a result, the experimentally observed T_c of 1.9 K for Sample 1 (see below) corresponds to $d = 1.41(K_2/\alpha T_{c0})^{1/2}$. This d value is comparable to the superconducting coherence length given by $\xi_{1,2}(0) = (K_{1,2}/\alpha T_{c0})^{1/2}$ for the anisotropic stripe, suggesting that the use of a δ -function is reasonably self-consistent given that the basic length for order parameter variation in the Ginzburg-Landau theory is $\xi_{1,2}(0)$.

The y -component of the order parameter, η_y , was found to first become non-zero for $T < T_c$ as shown in Fig. 1(d) (upper panel), making the dislocation a nucleation center for superconductivity. Below T_{c0} , both η_x and η_y are present, resulting in an enhanced order parameter near the dislocation [Fig. 1(d), lower panel]. The latter suggests that an edge dislocation in Sr_2RuO_4 is not a pinning center for Abrikosov vortices (see below) as opposed to that in high- T_c superconductors[21]. It is interesting to note that similar phenomenology can be obtained if two pairing states represented by a single-component order parameter have identical or very close intrinsic superconducting transition temperatures.

Experimentally, easily cleavable single crystals of Sr_2RuO_4 were synthesized by the floating-zone method. The bulk T_c was found to be 1.35 K without the presence of enhanced superconductivity (Supplemental Material Fig. 1), suggesting that very few, if any, Ru microdomains were present in our starting crystals. To overcome the unavailability of superconducting films of Sr_2RuO_4 in spite of an early report of initial synthesis success[22], we prepared single-crystal flakes with a lateral dimension of roughly 10 – 50 μm and a thickness of 300 – 800 nm by mechanical exfoliation. The flakes were transferred onto a Si/SiO₂ substrate with the c axis of the crystal perpendicular to the substrate. A standard four-point pattern was defined on the crystal via contact

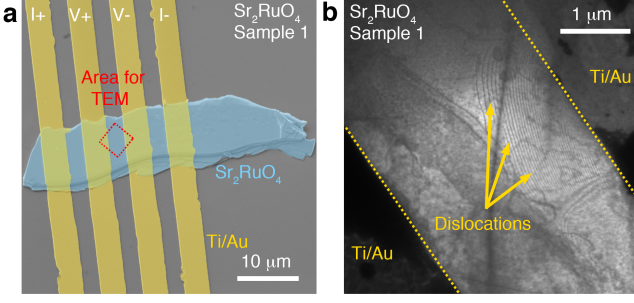


FIG. 2. (Color online) (a) False-color scanning electron microscopy (SEM) image of Sample 1. The red square indicates the area examined by TEM. (b) TEM image of the boxed area in (a), showing dislocation lines but no Ru microdomains. The region not shown in this image was also checked by SEM and TEM and found to possess no Ru microdomains.

photolithography, followed by a 30 s oxygen plasma operated at 100 mTorr and 100 W to remove any residue photoresist before metallization. Electrical leads of 50 nm Ti and 200 nm Au were then deposited at 45-degree angles with respect to the substrate norm to ensure the continuity of the leads on the side walls of the crystals, resulting in contact resistances less than 1Ω at low temperatures. Low temperature dc measurements were performed in a ^3He refrigerator with a base temperature of 0.35 K. The critical current was defined by the bias current corresponding to a voltage response of 50 nV.

Single-crystal flakes of Sr_2RuO_4 were examined by scanning electron microscopy (SEM) and transmission electron microscopy (TEM). Both dislocations and Ru microdomains were found in some flakes with Ru microdomains always locating at the edge of the crystal [Fig. 1(a)], perhaps because the cleaving tends to occur at the Ru/ Sr_2RuO_4 boundary due to different mechanical strengths of Ru and Sr_2RuO_4 . For some flakes, however, no traces of Ru microdomains were found. In particular, in a four-wire Sr_2RuO_4 device, Sample 1, no Ru microdomains were found in the SEM [Fig. 2(a)] and the TEM [Fig. 2(b)] images taken before and after the low-temperature measurements, respectively. Meanwhile, dislocations were observed between the two voltage leads. Superconductivity with an enhanced onset $T_c = 1.9$ K was found [Fig. 3(a)], directly linking the presence of dislocations and an enhancement of superconductivity in Sr_2RuO_4 . A set of symmetry reduction parameters of $m_1/|\mu| = -1.5$, $m_2/|\mu| = -1.5$, $|\mu|/\alpha = 0.4$, and $d/\xi_2(0) = 1.41$ characterizing the dislocation will give rise to $T_{ch} = 3$ K and $T_c = 1.9$ K in the phenomenological theory presented above.

The presence of multiple dislocations [Fig. 2(b)], which should be described by different sets of symmetry reduction parameters, suggests that multiple phases may be present in Sample 1. This is consistent with the multiple features observed in the $R(T)$ curve [Fig. 3(a)]. The

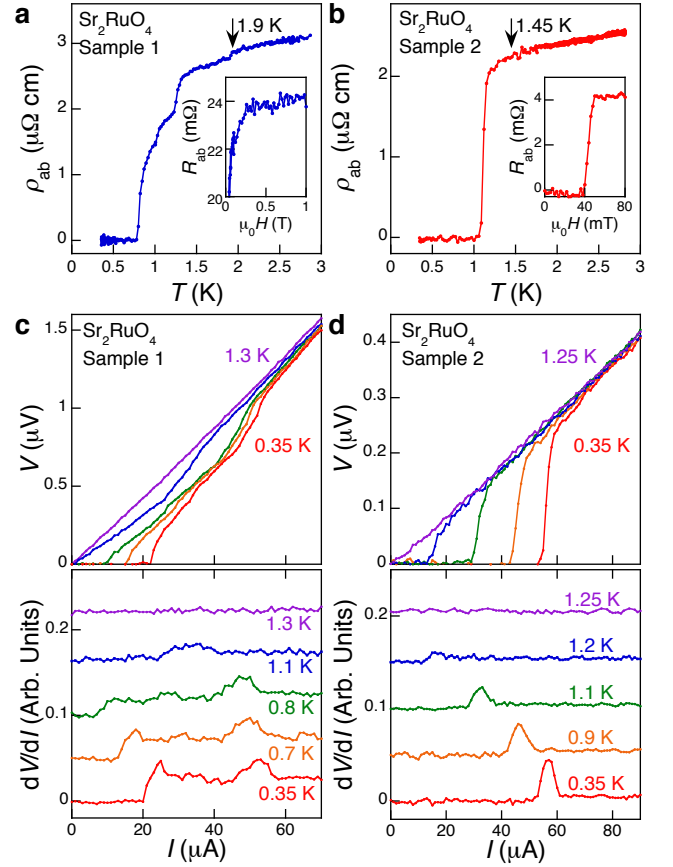


FIG. 3. (Color online) In-plane resistivity ρ_{ab} of (a) Sample 1 and (b) Sample 2 taken at zero applied magnetic field, plotted as a function of temperature. Insets: Magnetic field dependence of ρ_{ab} at 0.35 K, for field applied along the c axis. The upper critical field of Sample 1 was found to be about 0.3 T, suggesting the presence of enhanced superconductivity. Zero-field $V - I$ curves and corresponding $dV/dI - I$ curves at various temperatures for (c) Sample 1 showing multiple transitions and (d) Sample 2 showing a single transition. The $dV/dI - I$ curves except for those at 0.35 K were shifted for clarity.

voltage-current ($V - I$) characteristics and the $dV/dI - I$ curves were found to show double features suggesting the existence of two different phases at low temperatures [Fig. 3(c)], one corresponding to the dislocations and the other the bulk phase. In contrast, in Sample 2 (see SI Fig. 3 for the SEM image), a single onset T_c slightly lower than 1.5 K [Fig. 3(b)] and a single feature [Fig. 3(d)] were found in the $R(T)$, $V - I$, and $dV/dI - I$ curves, respectively.

The presence of dislocations in a type II superconductor is expected in general to enlarge the critical current density (J_c), which measures the strength of the vortex pinning, because Abrikosov vortices tend to be pinned to structural defects[23]. Essentially, the energy cost of placing a normal vortex core at a defect is in general smaller than the defect-free part of the sample, making

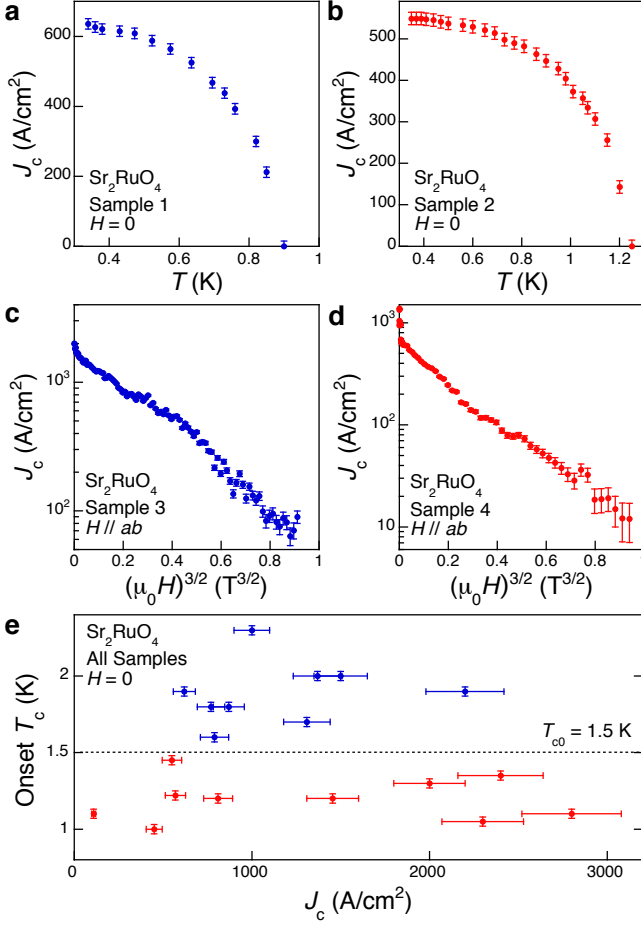


FIG. 4. (Color online) Zero-field critical current density J_c plotted as a function of temperature for (a) Sample 1 and (b) Sample 2. Base temperature (0.35 K) J_c plotted logarithmically as a function of $H^{3/2}$ for (c) Sample 3 and (d) Sample 4, showing roughly straight lines, consistent with the prediction of collective pinning theory. The magnetic field was applied parallel to the in-plane direction along some of the dislocation lines. (e) Onset T_c for samples with an enhanced T_c (Blue) and pure phase samples (Red) plotted as a function of their base temperature J_c at zero-field.

it a preferred site for vortex pinning. Strengthened vortex pinning due to dislocations was indeed reported in high- T_c superconductors[21]. For Sr_2RuO_4 , on the other hand, J_c would not be enhanced even when dislocations are present in the sample because a dislocation gives rise to locally enhanced rather than suppressed superconductivity. We would therefore expect samples with or without an enhanced T_c to show similar J_c values.

We measured J_c of our Sr_2RuO_4 flakes with an in-plane current (Fig. 4). Values of J_c were found to be much smaller than the depairing current density at the thermodynamic limit ($J_0 = cH_c/3\sqrt{6}\pi\lambda_{ab} = 5 \times 10^6$ A/cm², where $H_c = 20$ mT is the thermodynamic critical field and $\lambda_{ab} = 190$ nm the in-plane penetration depth), but larger than J_c values with the current applied along

the c axis measured previously in bulk Sr_2RuO_4 [24, 25]. As expected, the temperature and magnetic field dependences of J_c were found to be similar in samples with and without an enhanced T_c , showing that the presence of dislocations does not enhance vortex pinning. In addition, it was found that $J_c/J_0 \sim 10^{-4} - 10^{-3}$, indicating that the pinning potential is weak[23], and furthermore, $J_c(H) \sim \exp[-(H/H_0)^{3/2}]$ in the intermediate fields, consistent with that predicted by the collective pinning theory of vortex lattices[23]. The latter suggests that the vortices are pinned collectively by point defects instead of dislocations. Measurements on a large set of samples showed J_c values to fall into the same range regardless of whether a T_c enhancement was found in the sample [Fig. 4(e)], showing convincingly that dislocations are not pinning centers in Sr_2RuO_4 , as predicted by our phenomenological theory.

Useful insight into the mechanism of odd-parity superconductivity in Sr_2RuO_4 can be obtained by examining the microscopic origins of the T_c enhancement associated with a dislocation. An edge dislocation, as well as a screw dislocation, destroys locally both the four-fold rotational symmetry and layering along the c axis [Fig. 1(b)]. The topological nature of a dislocation demands that a number of the adjacent layers be placed locally closer than those in the bulk[26]. The local electronic states are then strongly restructured, becoming at the same time more three-dimensional (3D). Interestingly, the quantum oscillation measurements carried out under a hydrostatic pressure[27] suggest that the pressure, which lowers T_c of Sr_2RuO_4 , makes the Fermi surface more 2D like. Furthermore, applying a uniaxial pressure along the c axis of Sr_2RuO_4 , which should increase the interlayer coupling, was found to enhance T_c [28]. All these observations suggest that an enhanced T_c in Sr_2RuO_4 may originate from the strengthening of the interlayer scattering of electrons near a dislocation, which may also lead to a strongly p_z -dependent order parameter. Such a strongly p_z -dependent order parameter was obtained in a band-dependent superconductivity model for Sr_2RuO_4 [29], which, incidentally, results in a strongly suppressed depairing current[30], explaining naturally the small J_c values observed in Sr_2RuO_4 .

The authors acknowledge useful discussions with Y. Maeno, C. C. Tsuei, S. B. Chung and V. Varkaruk. The work at Penn State is supported by DOE under Grant No. DE-FG02-04ER46159. The nanofabrication part of the work is supported by Penn State MRI Nanofabrication Lab under NSF Cooperative Agreement 0335765, NNIN with Cornell University and under NSF DMR 0908700. The TEM images were obtained at the TEM facility at FSU, supported by the Florida State University Research Foundation, NSF-DMR-0654118 and the State of Florida. K. S. is supported by JQI-NSF-PFC. The work at Tulane is supported by NSF under DMR-0645305.

* liu@phys.psu.edu

- [1] Y. Maeno, H. Hashimoto, K. Yoshida, S. Nishizaki, T. Fujita, J. G. Bednorz, and F. Lichtenberg, *Nature* **372**, 532 (1994).
- [2] T. M. Rice and M. Sigrist, *J. Phys. Condens. Matter* **7**, L643 (1995).
- [3] G. Baskaran, *Physica B* **223-224**, 490 (1996).
- [4] A. P. Mackenzie and Y. Maeno, *Rev. Mod. Phys.* **75**, 657 (2003).
- [5] Y. Maeno, S. Kittaka, T. Nomura, S. Yonezawa, and K. Ishida, *J. Phys. Soc. Jpn.* **81**, 011009 (2012).
- [6] D. A. Ivanov, *Phys. Rev. Lett.* **86**, 268 (2001).
- [7] S. Das Sarma, C. Nayak, and S. Tewari, *Phys. Rev. B* **73**, 220502(R) (2006).
- [8] C. Nayak, S. H. Simon, A. Stern, M. Freedman, and S. Das Sarma, *Rev. Mod. Phys.* **80**, 1083 (2008).
- [9] K. D. Nelson, Z. Q. Mao, Y. Maeno, and Y. Liu, *Science* **306**, 1151 (2004).
- [10] G. M. Luke, Y. Fudamoto, K. M. Kojima, M. I. Larkin, J. Merrin, B. Nachumi, Y. J. Uemura, Y. Maeno, Z. Q. Mao, Y. Mori, H. Nakamura, and M. Sigrist, *Nature* **394**, 558 (1998).
- [11] J. Xia, Y. Maeno, P. T. Beyersdorf, M. M. Fejer, and A. Kapitulnik, *Phys. Rev. Lett.* **97**, 167002 (2006).
- [12] I. I. Mazin and D. J. Singh, *Phys. Rev. Lett.* **79**, 733 (1997).
- [13] T. Kuwabara and M. Ogata, *Phys. Rev. Lett.* **85**, 4586 (2000).
- [14] K. K. Ng and M. Sigrist, *Europhys. Lett.* **49**, 473 (2000).
- [15] T. Nomura and K. Yamada, *J. Phys. Soc. Jpn.* **69**, 3678 (2000).
- [16] S. Koikegami, Y. Yoshida, and T. Yanagisawa, *Phys. Rev. B* **67**, 134517 (2003).
- [17] Y. Maeno, T. Ando, Y. Mori, E. Ohmichi, S. Ikeda, S. NishiZaki, and S. Nakatsuji, *Phys. Rev. Lett.* **81**, 3765 (1998).
- [18] M. Sigrist and H. Monien, *J. Phys. Soc. Jpn.* **70**, 2409 (2001).
- [19] Y. A. Ying, Y. Xin, B. W. Clouser, E. Hao, N. E. Staley, R. J. Myers, L. F. Allard, D. Fobes, T. Liu, Z. Q. Mao, and Y. Liu, *Phys. Rev. Lett.* **103**, 247004 (2009).
- [20] A. P. Mackenzie, R. K. W. Haselwimmer, A. W. Tyler, G. G. Lonzarich, Y. Mori, S. Nishizaki, and Y. Maeno, *Phys. Rev. Lett.* **80**, 161 (1998).
- [21] F. Sandiumenge, T. Puig, J. Rabier, J. Plain, and X. Obradors, *Adv. Mater.* **12**, 375 (2000).
- [22] Y. Krockenberger, M. Uchida, K. S. Takahashi, M. Nakamura, M. Kawasaki, and Y. Tokura, *Appl. Phys. Lett.* **97**, 082502 (2010).
- [23] G. Blatter, M. V. Feigel'man, V. B. Geshkenbein, A. I. Larkin, and V. M. Vinokur, *Rev. Mod. Phys.* **66**, 1125 (1994).
- [24] J. Hooper, Z. Q. Mao, K. D. Nelson, Y. Liu, M. Wada, and Y. Maeno, *Phys. Rev. B* **70**, 014510 (2004).
- [25] J. Hooper, M. Zhou, Z. Q. Mao, Y. Liu, R. Perry, and Y. Maeno, *Phys. Rev. B* **73**, 132510 (2006).
- [26] Y. Ran, Y. Zhang, and A. Vishwanath, *Nature Phys.* **5**, 298 (2009).
- [27] D. Forsythe, S. R. Julian, C. Bergemann, E. Pugh, M. J. Steiner, P. L. Alireza, G. J. McMullan, F. Nakamura, R. K. W. Haselwimmer, I. R. Walker, S. S. Saxena, G. G. Lonzarich, A. P. Mackenzie, Z. Q. Mao, and Y. Maeno, *Phys. Rev. Lett.* **89**, 166402 (2002).
- [28] S. Kittaka, H. Taniguchi, S. Yonezawa, H. Yaguchi, and Y. Maeno, *Phys. Rev. B* **81**, 180510(R) (2010).
- [29] M. E. Zhitomirsky and T. M. Rice, *Phys. Rev. Lett.* **87**, 057001 (2001).
- [30] H. Y. Kee, Y. B. Kim, and K. Maki, *Phys. Rev. B* **70**, 052505 (2004).